The Influence of Swarm Topologies in Many-objective Optimization Problems

Diana Cristina Valencia-Rodríguez and Carlos A. Coello Coello[0000−0002−8435−680X]

CINVESTAV-IPN (Evolutionary Computation Group)
Av. IPN 2508, San Pedro Zacatenco
Ciudad de México, 07360, México
dvalencia@computacion.cs.cinvestav.mx
ccoello@cs.cinvestav.mx

Abstract. Particle Swarm Optimization (PSO) is a bio-inspired metaheuristic that has been successfully adopted for single- and multi-objective optimization. Several studies show that the way in which particles are connected with each other (the swarm topology) influences PSO's behavior. A few of these studies have focused on analyzing the influence of swarm topologies on the performance of Multi-objective Particle Swarm Optimizers (MOPSOs) using problems with two or three objectives. However, to the authors' best knowledge such studies have not been done so far for many-objective optimization problems. This paper provides an anlysis of the influence of the ring, star, lattice, wheel, and tree topologies on the performance of SMPSO (a well-known Pareto-based MOPSO) using many-objective problems. Based on these results, we also propose two MOPSOs that use a combination of topologies: SMPSO-SW and SMPSO-WS. Our experimental results show that SMPSO-SW is able to outperform SMPSO in most of the test problems adopted.

Keywords: Swarm topology · Particle Swarm Optimization · Multi-objective Particle Swarm Optimization · Multi-objective optimization · Many-objective optimization

1 Introduction

Particle Swarm Optimization (PSO) is a metaheuristic that simulates the movements of a flock of birds or a school of fish seeking food [8]. PSO adopts a swarm of particles that communicate with each other intending to find the optimal solution. It has been experimentally shown that the communication networks connecting the particles (the *swarm topology*) influence PSO's performance [7,11]. Therefore, selecting the right swarm topology is crucial for obtaining good solutions.

There are numerous extensions of PSO for solving multi-objective optimization problems (see for example [4,18,9,5,13]). However, there are few studies on the influence of swarm topologies on the performance of Multi-Objective Particle Swarm Optimizers (MOPSOs) and such studies only analyze problems with

three or fewer objectives [17,14,15]. Consequently, the influence of the swarm topology in the solution of many-objective problems remains as an unexplored topic.

In this paper, we analyze the influence of the ring, star, lattice, wheel, and tree topologies on the performance of the Speed-constrained Multiobjective Particle Swarm Optimizer (SMPSO) [12] using many-objective problems. In particular, we adopt the DTLZ1, DTLZ2, DTLZ3, DTLZ4, and DTLZ7 problems from the Deb-Thiele-Laumanns-Zitzler (DTLZ) [3] test suite with 3, 5, 8, and 10 objectives.[1] As will be seen later on, the results obtained show that the wheel and star topologies provide the best performance concerning the hypervolume and s-energy indicators. Based on these results, we propose here two new MOPSOs that use a combination of these two topologies: the SMPSO-SW and the SMPSO-WS. Our preliminary experimental results show that SMPSO-SW is very competitive with respect to the original SMPSO.

The remainder of this paper is organized in the following way. In Section 2, we provide a brief explanation of background concepts. Then, in Section 3, we explain what a swarm topology is, and we give some examples. After that, in Section 4, we discuss the functionality of SMPSO as well as the way in which we modified it for handling different swarm topologies. In Section 5, we present the results of our initial experiments. Based on these results, we propose two new MOPSOs described in Section 6. Finally, in Section 7, we provide our conclusions and some possible paths for future work.

2 Background

2.1 Multi-objective Optimization

In multi-objective optimization, the aim is to solve problems of the type[2]:

$$\text{minimize } \boldsymbol{f}(\boldsymbol{x}) := [f_1(\boldsymbol{x}), f_2(\boldsymbol{x}), \ldots, f_k(\boldsymbol{x})] \tag{1}$$

subject to:

$$g_i(\boldsymbol{x}) \leq 0 \quad i = 1, 2, \ldots, m \tag{2}$$

$$h_i(\boldsymbol{x}) = 0 \quad i = 1, 2, \ldots, p \tag{3}$$

where $\boldsymbol{x} = [x_1, x_2, \ldots, x_n]^T$ is the vector of decision variables, $f_i : \mathbb{R}^n \rightarrow \mathbb{R}$, $i = 1, ..., k$ are the objective functions and $g_i, h_j : \mathbb{R}^n \rightarrow \mathbb{R}$, $i = 1, ..., m$, $j = 1, ..., p$ are the constraint functions of the problem.

[1] Although many-objective problems are those having more than 3 objectives, our experiments include test problems with 3 objectives to allow a more clear visualization of the effect of dimensionality increase in objective function space.

[2] Without loss of generality, we will assume only minimization problems.

A few additional definitions are required to introduce the notion of optimality used in multi-objective optimization:

Definition 1. Given two vectors $\boldsymbol{x}, \boldsymbol{y} \in \mathbb{R}^k$, we say that $\boldsymbol{x} \leq \boldsymbol{y}$ if $x_i \leq y_i$ for $i = 1, ..., k$, and that $\boldsymbol{x}$ **dominates** $\boldsymbol{y}$ (denoted by $\boldsymbol{x} \prec \boldsymbol{y}$) if $\boldsymbol{x} \leq \boldsymbol{y}$ and $\boldsymbol{x} \neq \boldsymbol{y}$.

Definition 2. We say that a vector of decision variables $\boldsymbol{x} \in \mathcal{X} \subset \mathbb{R}^n$ is **nondominated** with respect to $\mathcal{X}$, if there does not exist another $\boldsymbol{x}' \in \mathcal{X}$ such that $\boldsymbol{f}(\boldsymbol{x}') \prec \boldsymbol{f}(\boldsymbol{x})$.

Definition 3. We say that a vector of decision variables $\boldsymbol{x}^* \in \mathcal{F} \subset \mathbb{R}^n$ ($\mathcal{F}$ is the feasible region) is **Pareto-optimal** if it is nondominated with respect to $\mathcal{F}$.

Definition 4. The **Pareto Optimal Set** $\mathcal{P}^*$ is defined by:

$$\mathcal{P}^* = \{\boldsymbol{x} \in \mathcal{F} | \boldsymbol{x} \text{ is Pareto-optimal}\}$$

Definition 5. The **Pareto Front** $\mathcal{PF}^*$ is defined by:

$$\mathcal{PF}^* = \{\boldsymbol{f}(\boldsymbol{x}) \in \mathbb{R}^k | \boldsymbol{x} \in \mathcal{P}^*\}$$

Therefore, our aim is to obtain the Pareto optimal set from the set $\mathcal{F}$ of all the decision variable vectors that satisfy (2) and (3).

In this paper, we address problems with more than three objectives (the so-called *many-objective optimization problems*).

2.2 Particle Swarm Optimization

PSO is a bio-inspired metaheuristic proposed by James Kennedy and Russel Eberhart in 1995 [8]. PSO operates with a *swarm* that is a set composed of potential solutions called *particles*. Each particle moves towards promising regions influenced by its previous best position and the best position found so far by the particles in the neighborhood.

Let $\mathbf{x_i}(t)$ be the position of a particle in generation t. Then, PSO updates its position using the following expression:

$$\mathbf{x_i}(t+1) = \mathbf{x_i}(t) + \mathbf{v_i}(t+1). \tag{4}$$

$\mathbf{v_i}(t+1)$ is known as the *velocity vector* and is defined by:

$$\mathbf{v_i}(t+1) = w\mathbf{v_i}(t) + C_1 r_1(\mathbf{x_{p_i}} - \mathbf{x_i}(t)) + C_2 r_2(\mathbf{x_{l_i}} - \mathbf{x_i}(t)) \tag{5}$$

where $r_1, r_2 \in U(0,1)$; C_1 and C_2 are positive constants called *cognitive* and *social* factors, respectively; and w is a positive parameter called *inertia weight*. The position $\mathbf{x}_{p_i}$ is the best solution found by the particle, and $\mathbf{x}_{l_i}$ is the best solution found by the particle's neighbors (known as *leader*). Each particle's neighborhood is determined by the *swarm topology*, which defines the connections of influence among particles.

3 Swarm Topologies

A swarm topology is a social network represented by a graph where each vertex is a particle, and there is an edge between two particles if they influence each other [11]. A topology can change along with the generations (*dynamic topology*) or remain static during the execution (*static topology*). Its formal definition is the following [10]:

Definition 1. *A* ***swarm topology*** *at generation i is a graph $T_i = (P_i, E_i)$ where the vertex set $P_i = \{p_0, p_1, ..., p_{n-1}\}$ is a set of particles.*

Many swarm topologies have been proposed over the years, each of which having different characteristics. For this study, we selected five static topologies which are representative of the state-of-the-art in the area [7,11]:

- **Lattice**. The graph of this topology represents a two-dimensional lattice. Each particle influences the neighbors above, below, and two on each side. See Fig. 1a.
- **Star** (*gbest*). Each particle in this topology influences the remaining particles in the swarm. See Fig. 1b.
- **Tree**. The particles in this topology are arranged hierarchically, resembling a tree. Each particle influences its father and its children, and viceversa. See Fig. 1c.
- **Wheel**. In this topology, a central particle influences the others in the swarm, and they influence it as well. See Fig. 1d.
- **Ring** (lbest). In this topology, each particle influences its two nearest neighbors. See Fig. 1e.

4 Multi-objective Particle Swarm Optimizer with a Topology Handling Scheme

A single-objective PSO updates the position $\mathbf{x_{p_i}}$ with the position $\mathbf{x_i}(t)$ at each generation if $f(\mathbf{x_i}(t))$ is better than $f(\mathbf{x_{p_i}})$. Then, PSO examines the personal best positions in the particle's neighborhood and selects its leader from it. In contrast, in multi-objective optimization, we often find incomparable solutions. Therefore, most of the MOPSOs store the best positions found so far in a separate set (called *external archive*) and take the leaders from it without specifying the particle's neighborhood.

We selected for the experimental analysis a standard Pareto-based MOPSO that works in this way, the SMPSO [12]. Its core idea is to control the particles' velocity employing a constriction factor χ that prevents high-velocity values and guarantees convergence under certain conditions [1]. This coefficient is defined by:

$$\chi = 2/(2 - \varphi - \sqrt{\varphi^2 - 4\varphi}) \tag{6}$$

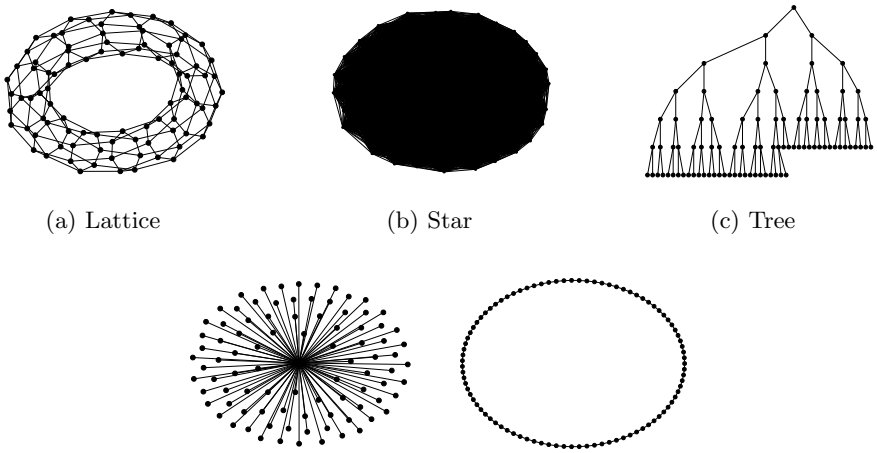

(a) Lattice (b) Star (c) Tree

(d) Wheel (e) Ring

Fig. 1. Swarm topologies of state of the art.

where

$$\varphi = \begin{cases} C_1 + C_2 & \text{if } C_1 + C_2 > 4 \\ 1 & \text{if } C_1 + C_2 \leq 4 \end{cases} \tag{7}$$

Moreover, SMPSO implements a mechanism to constrain the accumulated velocity of the particle i in the dimension j using the following expression:

$$v_{i,j}(t) = \begin{cases} \delta_j & \text{if } v_{i,j}(t) > \delta_j \\ -\delta_j & \text{if } v_{i,j}(t) \leq -\delta_j \\ v_{i,j}(t) & \text{otherwise} \end{cases} \tag{8}$$

where $\delta_j = (upper\_limit_j - lower\_limit_j)/2$, and the j^{th} decision variable is in the range $[lower\_limit_j, upper\_limit_j]$.

Therefore, the particles' velocity is computed using equation (5) and then the result is multiplied by the constriction factor defined in equation (6), and it is bounded using the rule defined in equation (8).

In general, SMPSO works in the following way. First, the swarm is initialized with random values, and the external archive is created with the non-dominated solutions of the swarm. Then, until a maximum number of generations is reached, each particle leader is selected by randomly taking two solutions from the external archive and selecting the one with the largest crowding distance, which measures how isolated is a solution from the others. Next, with the selected leaders, the velocity and position of the particles are computed. Moreover, polynomial-based mutation [2] is applied to the new particles using a probability p_m, and the resulting particles are evaluated. Finally, the personal best positions of the particles and the external archive are updated. If the external archive exceeds its

maximum number of elements, the element with the lowest crowding distance is removed.

In SMPSO (and in most of the MOPSOs), the particles stored in the external archive represent the best positions that have been found and, therefore, the corresponding leaders are selected from among them. This sort of leader selection scheme does not allow the use of different topologies, because the interaction with the external archive does not consider the particle's neighborhood. Therefore, it is necessary to use a different leader selection scheme in order to consider different swarm topologies in SMPSO.

In [15], we proposed two topology handling schemes that differ in the place from which the leaders are taken. **Scheme 1** examines the personal best position of the particles and selects the leaders from them. And **scheme 2** assigns the elements from the external archive to each of the particles. Then, the leader is selected by examining the external archive elements assigned to the particle's neighbors.

Here, we adopt scheme 2 in SMPSO (the resulting version is called SMPSO-E2) because this scheme had the best performance in the study reported in [15]. The difference between SMPSO and SMPSO-E2 is that at each generation, SMPSO-E2 assigns the external archive elements to each particle. The archive elements are assigned again if the archive size is smaller than the swarm size. Then, each particle's leader is selected by randomly taking two of its neighbors and picking the one that has the assigned element with the largest crowding distance. After that, the following steps are the same as in the original SMPSO.

5 Experimental Analysis

To carry out our experimental analysis, we compared SMPSO and SMPSO-E2 using the tree, lattice, star, ring, and wheel topologies. For that sake, we performed 30 independent runs of each MOP using the parameters shown in Table 1.

Table 1. Parameters of the MOPSOs adopted in this study

Parameter	Value
Archive size	300
Swarm size	300
Mutation probability (p_m)	$1/n$
Inertia weight (w)	0.1
Max number of generations	2500

We adopted the DTLZ1-DTLZ4 and DTLZ7 problems from the scalable Deb-Thiele-Laumanns-Zitzler (DTLZ) test suite [3]. We tested these problems with 3, 5, 8, and 10 objectives where the decision variables (n) are defined by $n = m + k - 1$ and m is the number of objectives. We used a value of $k = 5$ for DTLZ1, $k = 10$ for DTLZ2-4, and $k = 20$ for DTLZ7.

For assessing performance, we used the hypervolume [19] and s-energy [6] indicators. The hypervolume measures the size of the objective space covered by the approximated set, given a reference point. The larger the space covered, the better the approximation. Therefore, the aim is to maximize the hypervolume indicator. We used as reference points the worst objective function values obtained in the approximated sets for each problem, multiplied by 1.1. On the other hand, the s-energy indicator measures the uniform distribution of a set in a d-dimensional manifold. A lower s-energy value implies an approximation set with higher diversity. Moreover, to evaluate the results' statistical confidence, we applied the Wilcoxon signed-rank test with a significance level of 5%.

Tables 2 and 3 present the mean and the standard deviation of the hypervolume and s-energy indicators. The best values have a gray background, and the symbol "*" means that the difference of the corresponding algorithm with respect to the others is statistically significant.

Table 2. Mean and standard deviation of hypervolume indicator for SMPSO and SMPSO-E2. The best values have a gray background, and the symbol "*" indicates that the result is statistically significant.

	m	SMPSO	SMPSO-E2				
			Lattice	Star	Tree	Wheel	Ring
DTLZ1	3	1.3992e-1 (2.3e-4)	1.4008e-1 (2.5e-4)	1.3999e-1 (2.3e-4)	1.4007e-1 (2.8e-4)	*1.4077e-1 (4.7e-4)	1.4017e-1 (2.9e-4)
	5	7.349e-2 (6.1e-4)	7.4196e-2 (5.1e-4)	7.3538e-2 (4.5e-4)	7.4221e-2 (4.9e-4)	*7.5724e-2 (4.2e-4)	7.4519e-2 (6.1e-4)
	8	2.4274e+12 (7.0e+8)	2.4276e+12 (6.5e+5)	2.4276e+12 (1.0e+7)	2.4276e+12 (1.5e+6)	*2.4276e+12 (1.8e+5)	2.4275e+12 (3.1e+7)
	10	3.6423e+16 (0.e+0)	3.6423e+16 (1.3e+11)	3.6423e+16 (3.6e+9)	3.6423e+16 (1.3e+11)	3.6423e+16 (1.1e+10)	3.6409e+16 (7.5e+13)
DTLZ2	3	9.8288e-1 (2.4e-3)	9.8372e-1 (2.4e-3)	9.8330e-1 (3.e-3)	9.8388e-1 (2.e-3)	*9.8831e-1 (2.9e-3)	9.8334e-1 (2.3e-3)
	5	8.3629e+1 (8.0e-2)	8.3699e+1 (7.8e-2)	8.3619e+1 (8.7e-2)	8.3701e+1 (1.e-1)	*8.4043e+1 (3.4e-2)	8.3682e+1 (6.6e-2)
	8	7.2833e+3 (8.6e+0)	7.2976e+3 (5.4e+0)	7.2836e+3 (1.1e+1)	7.2930e+3 (6.9e+0)	*7.3311e+3 (1.3e+0)	7.2945e+3 (6.5e+0)
	10	1.7587e+5 (4.3e+2)	1.7623e+5 (2.0e+2)	1.7585e+5 (4.4e+2)	1.7618e+5 (2.1e+2)	*1.7688e+5 (5.6e+1)	1.7632e+5 (1.5e+2)
DTLZ3	3	1.0220e+0 (2.e-3)	1.0230e+0 (2.6e-3)	1.0219e+0 (2.2e-3)	1.0230e+0 (3.1e-3)	*1.0287e+0 (3.3e-3)	1.0236e+0 (2.5e-3)
	5	1.5944e+10 (0.e+0)	1.5944e+10 (0.e+0)	1.5944e+10 (0.e+0)	1.5944e+10 (0.e+0)	1.5944e+10 (0.e+0)	1.5944e+10 (0.e+0)
	8	2.9538e+24 (7.e+17)	2.9538e+24 (8.5e+17)	2.9538e+24 (6.6e+17)	2.9538e+24 (8.1e+17)	*2.9538e+24 (0.e+0)	2.9538e+24 (9.7e+17)
	10	9.5943e+30 (7.7e+23)	9.5943e+30 (1.e+24)	9.5943e+30 (8.5e+23)	9.5943e+30 (1.1e+24)	*9.5943e+30 (2.3e+15)	9.5943e+30 (1.4e+24)
DTLZ4	3	1.1089e+0 (1.9e-3)	1.1082e+0 (2.1e-3)	1.1092e+0 (2.2e-3)	1.1082e+0 (2.2e-3)	*1.1159e+0 (2.9e-3)	1.108e+0 (2.5e-3)
	5	7.7119e+1 (2.3e-2)	7.7087e+1 (1.9e-2)	7.7113e+1 (2.1e-2)	7.7098e+1 (2.2e-2)	*7.7139e+1 (2.7e-2)	7.7083e+1 (2.2e-2)
	8	1.4538e+4 (7.2e-1)	1.4537e+4 (1.5e+0)	1.4538e+4 (6.9e-1)	1.4537e+4 (1.2e+0)	1.4537e+4 (2.3e+0)	1.4536e+4 (1.5e+0)
	10	3.4448e+5 (1.3e+1)	3.4438e+5 (7.7e+1)	3.4448e+5 (1.3e+1)	3.444e+5 (5.6e+1)	3.4415e+5 (5.4e+2)	3.443e+5 (1.7e+2)
DTLZ7	3	2.595e+0 (9.4e-3)	2.5939e+0 (1.1e-2)	2.5937e+0 (5.6e-3)	2.593e+0 (1.2e-2)	2.5981e+0 (1.3e-2)	2.5952e+0 (7.9e-3)
	5	4.0609e+0 (4.5e-2)	4.0549e+0 (5.7e-2)	4.0451e+0 (8.6e-2)	4.0871e+0 (5.9e-2)	*4.2474e+0 (5.8e-2)	4.0565e+0 (6.6e-2)
	8	6.3453e+0 (1.4e-1)	6.4385e+0 (1.2e-1)	6.2954e+0 (1.7e-1)	6.4785e+0 (1.1e-1)	*7.0286e+0 (8.2e-2)	6.4752e+0 (1.1e-1)
	10	3.7925e+1 (3.8e+0)	3.8882e+1 (7.9e-1)	3.8786e+1 (2.2e-1)	3.9125e+1 (1.8e-1)	*3.9788e+1 (2.7e-1)	3.9112e+1 (1.9e-1)

Table 2 shows that, on average, the wheel topology has the best performance for the hypervolume indicator in all of the objectives. In comparison, the star topology performs worst. Regarding the other topologies, the tree topology performs better than the lattice, and the lattice topology performs better than the ring. We validated in [16] the topologies' obtained arrangement using the Wilcoxon signed-rank test with a significance level of 5%. Therefore, it seems that the lower the degree of connectivity the topology has, the better the hypervolume value. Compared with SMPSO, the SMPSO-E2 with wheel topology performed better in almost all problems.

Conversely, Table 3 shows that the star topology had the best performance on average in all of the problems regarding the s-energy indicator; and the wheel topology had the worst performance. If we compare the topologies with the original SMPSO, the SMPSO-E2 with the star topology performed better than

Table 3. Mean and standard deviation of s-energy indicator for SMPSO and SMPSO-E2. The best values have a gray background, and the symbol "*" indicates that the result is statistically significant.

	m	SMPSO	SMPSO-E2				
			Lattice	Star	Tree	Wheel	Ring
DTLZ1	3	6.1494e+8 (2.7e+8)	7.1795e+8 (2.3e+8)	*6.0124e+8 (5.4e+8)	6.2656e+8 (1.4e+8)	1.2194e+9 (3.7e+8)	6.3859e+8 (1.3e+8)
	5	3.7068e+10 (2.3e+10)	5.4841e+10 (2.3e+10)	2.8204e+10 (1.8e+10)	6.4885e+10 (2.8e+10)	2.5939e+11 (8.2e+10)	8.9301e+10 (3.1e+10)
	8	2.1012e+11 (6.5e+11)	2.3178e+11 (2.3e+11)	1.3365e+11 (3.1e+11)	2.1332e+11 (2.5e+11)	1.4822e+12 (9.5e+11)	3.1467e+11 (3.6e+11)
	10	7.3677e+10 (2.4e+11)	1.8238e+11 (2.8e+11)	9.4263e+11 (3.2e+12)	2.8388e+11 (5.9e+11)	3.4625e+12 (5.6e+12)	3.0778e+11 (5.7e+11)
DTLZ2	3	7.6337e+9 (8.5e+9)	2.148e+10 (5.e+9)	9.1892e+9 (9.1e+9)	2.0046e+10 (6.3e+8)	2.1769e+10 (7.3e+9)	2.0061e+10 (2.5e+7)
	5	3.6556e+10 (2.3e+10)	9.1259e+10 (4.3e+10)	2.9936e+10 (2.1e+10)	1.2281e+11 (3.2e+10)	1.3777e+11 (1.3e+10)	1.4109e+11 (2.3e+10)
	8	9.6620e+10 (4.8e+10)	1.6801e+11 (6.6e+10)	7.7822e+10 (3.3e+10)	2.1695e+11 (9.2e+10)	6.0208e+11 (8.6e+10)	3.2113e+11 (1.1e+11)
	10	1.7591e+11 (5.2e+10)	2.8241e+11 (8.3e+10)	1.9251e+11 (5.7e+10)	2.9815e+11 (8.1e+10)	9.5665e+11 (1.4e+11)	4.5666e+11 (1.6e+11)
DTLZ3	3	8.3273e+9 (8.3e+9)	1.8324e+10 (4.8e+9)	8.6146e+9 (8.6e+9)	1.9597e+10 (2.7e+9)	2.1457e+10 (7.2e+9)	2.0907e+10 (3.7e+9)
	5	7.7074e+9 (1.4e+10)	3.1648e+10 (2.8e+10)	2.8588e+9 (6.1e+9)	5.1345e+10 (3.7e+10)	1.4193e+11 (2.2e+10)	9.0929e+10 (5.e+10)
	8	8.7195e+9 (1.7e+10)	1.0675e+10 (1.2e+10)	5.3661e+9 (1.0e+10)	2.2667e+10 (3.8e+10)	6.3975e+10 (1.6e+11)	2.4668e+10 (3.3e+10)
	10	1.6612e+10 (2.2e+10)	2.6718e+10 (3.3e+10)	1.0395e+10 (1.6e+10)	2.2187e+10 (2.4e+10)	1.5392e+10 (1.5e+10)	2.7334e+10 (4.1e+10)
DTLZ4	3	1.2133e+10 (1.3e+10)	2.0457e+10 (1.9e+9)	1.519e+10 (8.3e+9)	2.0117e+10 (2.e+8)	2.0134e+10 (2.4e+8)	2.01e+10 (1.6e+8)
	5	8.4434e+10 (3.5e+10)	1.6135e+11 (3.1e+10)	8.3891e+10 (3.e+10)	1.5889e+11 (2.7e+10)	1.6925e+11 (3.1e+10)	1.7089e+11 (2.6e+10)
	8	2.8836e+11 (7.0e+10)	2.8382e+11 (7.2e+10)	2.6838e+11 (7.1e+10)	3.0473e+11 (8.e+10)	5.8014e+11 (3.6e+11)	3.6321e+11 (1.1e+11)
	10	4.6999e+11 (8.2e+10)	4.4684e+11 (8.6e+10)	4.5576e+11 (1.1e+11)	4.4513e+11 (9.1e+10)	4.3781e+11 (1.8e+11)	4.9120e+11 (1.4e+11)
DTLZ7	3	4.3088e+7 (1.1e+7)	7.2996e+8 (3.6e+9)	4.9655e+7 (3.7e+7)	6.3745e+7 (7.4e+7)	1.3143e+9 (4.3e+9)	7.1740e+8 (3.6e+9)
	5	7.8658e+8 (2.1e+9)	7.4775e+8 (1.2e+9)	1.9315e+9 (5.e+9)	4.8294e+9 (7.7e+9)	1.4197e+10 (1.2e+10)	3.5381e+9 (5.6e+9)
	8	3.1266e+10 (2.6e+10)	7.0838e+10 (3.4e+10)	2.5010e+10 (2.3e+10)	9.037e+10 (5.2e+10)	4.0819e+11 (1.2e+11)	9.6846e+10 (4.6e+10)
	10	5.7154e+10 (4.5e+10)	1.4790e+11 (7.0e+10)	5.9874e+10 (3.2e+10)	1.8519e+11 (8.9e+10)	1.1722e+12 (3.4e+11)	1.8915e+11 (7.5e+10)

the original SMPSO in more problems. However, the Wilcoxon test did not show a statistical significance of the results and in [16] we could not define a statistically confident arrangement between all the topologies.

In summary, we can see that the wheel topology had the best performance regarding the hypervolume indicator and the star topology had the best performance concerning the s-energy indicator. The results also show that there could be a relationship between the degree of connectivity and the hypervolume values.

6 Combining Topologies

The previous experiments showed that the wheel topology had the best performance with respect to the hypervolume indicator. In contrast, the star topology performed best with respect to the s-energy indicator. Therefore, it can be easily inferred that the wheel topology promotes the MOPSO's convergence, and that the star topology improves the solution's distribution. Thus, if we use both topologies, we could balance the exploration and exploitation of the SMPSO-E2.

In order to validate this hypothesis, we modified the SMPSO-E2 to use a dynamic topology that adopts one topology the first half of the generations and changes to another one for the second half of the generations. The version of SMPSO-E2 that uses the wheel topology the first half of the genrations and the star topology during the second half is called SMPSO-WS. Furthermore, the SMPSO-E2 that uses star topology during the first half of the generations and the wheel topology during the second half is called SMPSO-SW.

We performed 30 independent runs of SMPSO, SMPSO-WS, and SMPSO-SW with the parameters and problems that we used in the previous experimental study. For assessing performance, we used again the hypervolume (with the same reference points) and s-energy indicators.

Tables 4 and 5 show the mean and standard deviation of the hypervolume and s-energy indicator. The "*" symbol means that the difference between the corresponding algorithm and the others is statistically significant.

Table 4. Mean and standard deviation of hypervolume indicator for SMPSO, SMPSO-WS, and SMPSO-SW. The best values have a gray background, and the symbol "*" indicates that the result is statistically significant.

	m	SMPSO	SMPSO-WS	SMPSO-SW
DTLZ1	3	1.3992e-1 (2.3e-4)	1.4004e-1 (2.1e-4)	*1.4056e-1 (4.6e-4)
	5	7.349e-2 (6.1e-4)	7.3924e-2 (4.6e-4)	*7.5737e-2 (2.5e-4)
	8	2.4274e+12 (7.0e+8)	2.4276e+12 (5.6e+5)	2.4276e+12 (4.1e+6)
	10	3.6423e+16 (0.e+0)	3.6423e+16 (0.e+0)	3.6423e+16 (1.8e+9)
DTLZ2	3	9.8288e-1 (2.4e-3)	9.8370e-1 (2.7e-3)	*9.8981e-1 (2.7e-3)
	5	8.3629e+1 (8.0e-2)	8.3745e+1 (8.1e-2)	*8.4007e+1 (6.6e-2)
	8	7.2833e+3 (8.6e+0)	7.3003e+3 (5.e+0)	*7.3293e+3 (3.1e+0)
	10	1.7587e+5 (4.3e+2)	1.7637e+5 (1.3e+2)	*1.7681e+5 (7.7e+1)
DTLZ3	3	1.0220e+0 (2.e-3)	1.0228e+0 (2.0e-3)	*1.0281e+0 (3.7e-3)
	5	1.5944e+10 (0.e+0)	1.5944e+10 (0.e+0)	1.5944e+10 (0.e+0)
	8	2.9538e+24 (7.e+17)	2.9538e+24 (3.4e+17)	*2.9538e+24 (0.e+0)
	10	9.5943e+30 (7.7e+23)	9.5943e+30 (4.9e+23)	*9.5943e+30 (1.8e+23)
DTLZ4	3	1.1089e+0 (1.9e-3)	1.1089e+0 (2.1e-3)	*1.1140e+0 (2.9e-3)
	5	7.7119e+1 (2.3e-2)	7.7119e+1 (2.e-2)	*7.7142e+1 (2.4e-2)
	8	*1.4538e+4 (7.2e-1)	1.4538e+4 (7.2e-1)	1.4537e+4 (1.6e+0)
	10	*3.4448e+5 (1.3e+1)	3.4445e+5 (2.9e+1)	3.4431e+5 (1.5e+2)
DTLZ7	3	2.595e+0 (9.4e-3)	2.5919e+0 (8.7e-3)	2.5958e+0 (1.1e-2)
	5	4.0609e+0 (4.5e-2)	4.0212e+0 (6.1e-2)	*4.2420e+0 (6.3e-2)
	8	6.3453e+0 (1.4e-1)	6.3408e+0 (1.3e-1)	*7.0338e+0 (1.1e-1)
	10	3.7925e+1 (3.8e+0)	3.8854e+1 (2.6e-1)	*3.9817e+1 (1.6e-1)

Regarding the hypervolume indicator, it is clear that SMPSO-SW performs best in almost all of the test problems. We assume that this happened because the algorithm examines new regions in the search space at the beginning of the search with the star topology; consequently, the algorithm seems to be able to find promising regions of the search space, which makes it a very successful approach. Then, it exploits these promising regions using the wheel topology, obtaining a refined solution. In contrast, the SMPSO-WS tries two exploit a non-promising region using the wheel topology and then moves to many regions using the star topology thus preventing the algorithm from converging.

In the case of the s-energy indicator, the SMPSO performs best in almost all of the problems. Therefore, neither the SMPSO-WS nor SMPSO-SW had enough impact on this indicator.

Table 5. Mean and standard deviation of s-energy indicator for SMPSO, SMPSO-WS and SMPSO-SW. The best values have a gray background, and the symbol "*" indicates that the result is statistically significant.

	m	SMPSO	SMPSO-WS	SMPSO-SW
DTLZ1	3	6.1494e+8 (2.7e+8)	1.2030e+9 (3.6e+9)	1.1281e+9 (2.3e+8)
	5	3.7068e+10 (2.3e+10)	3.3739e+10 (1.7e+10)	2.1303e+11 (8.6e+10)
	8	*2.1012e+11 (6.5e+11)	2.4204e+11 (1.9e+11)	1.3907e+12 (6.6e+11)
	10	*7.3677e+10 (2.4e+11)	3.3888e+11 (6.8e+11)	4.9779e+12 (4.7e+12)
DTLZ2	3	*7.6337e+9 (8.5e+9)	2.09e+10 (3.5e+9)	2.0074e+10 (4.7e+7)
	5	*3.6556e+10 (2.3e+10)	1.3925e+11 (1.8e+10)	1.3772e+11 (1.8e+10)
	8	*9.6620e+10 (4.8e+10)	4.5010e+11 (3.0e+10)	5.6628e+11 (8.1e+10)
	10	*1.7591e+11 (5.2e+10)	7.123e+11 (9.0e+10)	8.4480e+11 (8.7e+10)
DTLZ3	3	*8.3273e+9 (8.3e+9)	1.9799e+10 (1.6e+9)	2.3675e+10 (1.1e+10)
	5	*7.7074e+9 (1.4e+10)	6.7153e+10 (4.4e+10)	9.3200e+10 (4.6e+10)
	8	8.7195e+9 (1.7e+10)	1.224e+10 (2.6e+10)	6.5998e+10 (2.7e+11)
	10	1.6612e+10 (2.2e+10)	1.3346e+10 (2.4e+10)	1.4024e+10 (1.6e+10)
DTLZ4	3	*1.2133e+10 (1.3e+10)	2.0995e+10 (3.8e+9)	2.1590e+10 (7.2e+9)
	5	*8.4434e+10 (3.5e+10)	1.2783e+11 (4.4e+10)	1.5963e+11 (3.1e+10)
	8	2.8836e+11 (7.0e+10)	2.6689e+11 (5.9e+10)	4.7546e+11 (1.3e+11)
	10	4.6999e+11 (8.2e+10)	4.6444e+11 (9.7e+10)	5.4920e+11 (2.7e+11)
DTLZ7	3	4.3088e+7 (1.1e+7)	4.8593e+7 (2.3e+7)	1.6039e+9 (4.3e+9)
	5	7.8658e+8 (2.1e+9)	5.3764e+8 (7.4e+8)	1.1789e+10 (1.1e+10)
	8	3.1266e+10 (2.6e+10)	3.0083e+10 (1.9e+10)	4.8259e+11 (1.6e+11)
	10	5.7154e+10 (4.5e+10)	6.5817e+10 (3.7e+10)	1.1618e+12 (2.9e+11)

7 Conclusions and Future Work

In this work, we analyzed the influence of the star, ring, wheel, lattice, and tree topologies on the performance of MOPSOs. The experimental results showed a relationship between the connectivity degree of topologies and the hypervolume values. If the connectivity degree decreases, the hypervolume value will increase.

The experimental results also showed that the wheel topology causes better values of the hypervolume indicator. In contrast, the star topology produces better values of the s-energy indicator. Hence, the wheel topology promotes the MOPSO's convergence, and the star topology improves the solution's distribution.

Therefore, in order to balance the exploitation and exploration of SMPSO-E2, we proposed two MOPSOs that use a combination of the wheel and star topologies: the SMPSO-WS and the SMPSO-SW. The SMPSO-SW outperformed the original SMPSO in most of the test problems adopted regarding the hypervolume indicator.

As part of our future work, we plan to test an adaptative topology that changes its connectivity degree depending on the behavior of the MOPSO.

Acknowledgements

The first author acknowledges support from CONACyT and CINVESTAV-IPN to pursue graduate studies in Computer Science. The second author acknowledges support from CONACyT grant no. 1920 and from a SEP-Cinvestav grant (application no. 4).

References

1. Clerc, M., Kennedy, J.: The Particle Swarm - Explosion, Stability, and Convergence in a Multidimensional Complex Space. 2002 IEEE Transactions on Evolutionary Computation (CEC 2002) **6**(1), 58–73 (2002)
2. Deb, K., Agrawal, R.B.: Simulated Binary Crossover for Continuous Search Space. Complex Systems **9**, 115–148 (1995)
3. Deb, K., Thiele, L., Laumanns, M., Zitzler, E.: Scalable Test Problems for Evolutionary Multiobjective Optimization. In: Abraham, A., Jain, L., Goldberg, R. (eds.) Evolutionary Multiobjective Optimization: Theoretical Advances and Applications, pp. 105–145. Springer London, London (2005)
4. Figueiredo, E.M.N., Ludermir, T.B., Bastos-Filho, C.J.A.: Many Objective Particle Swarm Optimization. Information Sciences **374**, 115–134 (December 20 2016)
5. Han, H., Lu, W., Zhang, L., Qiao, J.: Adaptive Gradient Multiobjective Particle Swarm Optimization. IEEE Transactions on Cybernetics **48**(11), 3067–3079 (November 2018)
6. Hardin, D., Saff, E.: Discretizing Manifolds via Minimum Energy Points. Notices of the American Mathematical Society **51**(10), 1186–1194 (2004)
7. Kennedy, J.: Small Worlds and Mega-Minds: Effects of Neighborhood Topology on Particle Swarm Performance. In: Proceedings of the 1999 Congress on Evolutionary Computation (CEC'1999). vol. 3, pp. 1931–1938 (Jul 1999)
8. Kennedy, J., Eberhart, R.: Particle Swarm Optimization. In: Proceedings of the 1995 IEEE International Conference on Neural Networks (ICNN 1995). vol. 4, pp. 1942–1948 (1995)
9. Lin, Q., Liu, S., Zhu, Q., Tang, C., Song, R., Chen, J., Coello Coello, C.A., Wong, K.C., Zhang, J.: Particle Swarm Optimization with a Balanceable Fitness Estimation for Many-Objective Optimization Problems. IEEE Transactions on Evolutionary Computation **22**(1), 32–46 (February 2018)
10. McNabb, A., Gardner, M., Seppi, K.: An Exploration of topologies and communication in large particle swarms. In: 2009 IEEE Congress on Evolutionary Computation (CEC 2009). pp. 712–719 (May 2009)
11. Mendes, R.: Population topologies and their influence in particle swarm performance. Ph.D. thesis, Departamento de Informática, Escola de Engenharia, Universidade do Minho (Apr 2004)
12. Nebro, A.J., Durillo, J.J., García-Nieto, J., Coello Coello, C.A., Luna, F., Alba, E.: SMPSO: A new PSO-based Metaheuristic for Multi-objective Optimization . In: 2009 IEEE Symposium on Computational Intelligence in Multi-Criteria Decision-Making (MCDM 2009). pp. 66–73 (Mar 2009)
13. Pan, A., Wang, L., Guo, W., Wu, Q.: A Diversity Enhanced Multiobjective Particle Swarm Optimization. Information Sciences **436**, 441–465 (April 2018)
14. Taormina, R., Chau, K.: Neural Network River Forecasting with Multi-objective Fully Informed Particle Swarm Optimization. Journal of Hydroinformatics **17**(1), 99–113 (2014)

15. Valencia-Rodríguez, D.C., Coello Coello, C.A.: A Study of Swarm Topologies and Their Influence on the Performance of Multi-Objective Particle Swarm Optimizers. In: Bäck, T., Preuss, M., Deutz, A., Wang, H., Doerr, C., Emmerich, M., Trautmann, H. (eds.) Parallel Problem Solving from Nature – PPSN XVI. pp. 285–298. Springer International Publishing (2020)
16. Valencia-Rodríguez, D.C.: Estudio de topologías cumulares y su impacto en el desempeño de un optimizador mediante cúmulos de partículas para problemas multiobjetivo. Master's thesis, Departamento de Computación, CINVESTAV-IPN, México (October 2019), `http://delta.cs.cinvestav.mx/~ccoello/tesis/tesis-valencia.pdf.gz`
17. Yamamoto, M., Uchitane, T., Hatanaka, T.: An Experimental Study for Multi-objective Optimization by Particle Swarm with Graph Based Archive. In: Proceedings of SICE Annual Conference (SICE 2012). pp. 89–94 (Aug 2012)
18. Zhu, Q., Lin, Q., Chen, W., Wong, K.C., Coello Coello, C.A., Li, J., Chen, J., Zhang, J.: An External Archive-Guided Multiobjective Particle Swarm Optimization Algorithm. IEEE Transactions on Cybernetics **49**(9), 2794–2808 (September 2017)
19. Zitzler, E.: Evolutionary Algorithms for Multiobjective Optimization: Methods and Applications. Ph.D. thesis, Swiss Federal Institute of Technology (ETH), Zurich, Suiza (Nov 1999)